

## Electronic supplementary information

### An electrochemical sensor for selective TNT sensing based on *Tobacco mosaic virus-like particle* binding agents

Faheng Zang<sup>a</sup>, Konstantinos Gerasopoulos<sup>a</sup>, Xiao Zhu Fan<sup>a</sup>, Adam Brown<sup>b</sup>, James Culver<sup>c</sup>  
and Reza Ghodssi\*<sup>a</sup>

<sup>a</sup> Department of Electrical and Computer Engineering, Institute for System Engineering

<sup>b</sup> Fischell Department of Bioengineering

<sup>c</sup> Institute for Bioscience and Biotechnology Research, Department of Plant Science and Landscape Architecture  
University of Maryland, College Park, USA.

Fax: +1 301 405 8158; Tel: +1 301 405 8158; E-mail: ghodssi@umd.edu

#### Genetic modification and purification of VLP binding agents

The Tobacco mosaic virus-like particle (VLP) coat protein gene was modified by PCR-based mutagenesis using a primer that augmented the gene with a bacterially optimized sequence coding for the 12-amino acid 2,4,6-trinitrotoluene (TNT) binding peptide WHWQRPLMPVSI at the C-terminus. The augmented coat protein gene did not produce full-length rods when subcloned into the pET21a bacterial vector and expressed in the BL21(DE3) bacterial expression system, possibly due to steric hindrance between adjacent coat proteins. To compensate for this, an amber stop codon was introduced between the 3' end of the VLP coat protein gene and the coding sequence for the TNT binding peptide<sup>S1</sup> (Fig. S1). This construct was subcloned into the pET21a expression vector and transformed into the JM109(DE3) bacterial expression system, containing the *supE44* gene, which produces a tRNA that competes with the terminal TAG amber stop codon, allowing random read-throughs of the full, augmented coat protein<sup>S2</sup>. This produced a mixture of unaugmented and augmented coat proteins that self-assemble into nanorod structured VLP-bp-TNT agents.

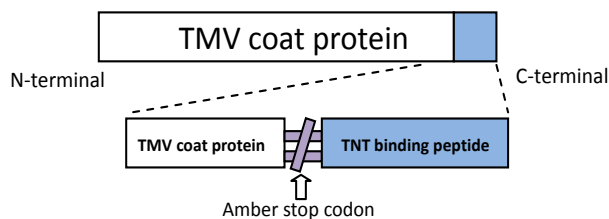


**Fig.S1.** TMV coat protein genetic modifications and configuration

And the nucleic acid sequence of the VLP-bp-TNT coat protein gene is

ATGTCGTGTTATAGCATTACCACCCCGTCGCAATTTGTGTTTCTGTCGAGCGCCTGGGCT  
 GACCCGATTGAACTGATTAACCTGTGTACCAACGCTCTGGGCAATCAGTTTCAAACCC  
 AGCAAGCGCGTACGGTGGTTCAGCGCCAATTCAGCCAGGTCTGGAAACCGTCTCCGC  
 AAGTCACCGTGCGTTTTCCGGATAGCGACTTCAAAGTTTATCGCTACAACGCCGTTCTG  
 AATCCGCTGGTCACCGCACTGCTGGGTGCTTTTGATACGCGTAACCGCATTATCGAAGT  
 GGAAAACCAGGCGAATCCGACCACCGCGGAAACCCTGGATGCAACCCGTCGCGTGGA  
 TGACGCGACCGTTGCCATTCGTAGTGCATCAACAATCTGATTGTTGAACTGATCCGCG  
 GCACGGGTTCTATAATCGTTCTTCGTTTGAATCGTCGTCGGGCCTGGTGTGGACCTCT  
 GGTCCGGCAACCTAGTGGCATTGGCAGCGTCCGCTTATGCCGGTATCTATTAA

The amino acid sequence of the VLP-bp-TNT coat protein is

MSCYSITTPSQFVFLSSAWADPIELINLCTNALGNQFQTQQARTVVQRQFSQVWKPSQVVT  
 VRFPDSDFKVYRYNAVLNPLVTALLGAFDTRNRIIEVENQANPTTAETLDATRRVDDATVA  
 IRSAINNLIVELIRGTGSYNRSSFESSSGLVWTSGPAT\*WHWQRPLMPVSI\*

The asterisks indicate stop codons.

### Characterization of diffusion coefficients using the Cottrell equation

The Cottrell equation describes the current-time equation of chronoamperometry, where the electrochemical current is recorded while a step function of potential is applied. It can be expressed as<sup>S3</sup>,

$$i_F(t) = nFAC(D / \pi t)^{1/2} \quad (1)$$

where  $i_F$  is the Faradaic current,  $n$  is the number of electrons involved in the reaction ( $n=4$  for the first reduction current peak of TNT),  $F$  is the Faraday constant,  $A$  is the area of the electrode ( $A=1 \times 10^{-5} \text{m}^2$ ),  $C$  is the concentration of TNT in the bulk ( $C=0.088 \text{mol/m}^3$ ),  $D$  is the diffusion coefficient ( $\text{m}^2/\text{s}$ ), and  $t$  is the time.

To calculate the diffusion coefficient in the electrochemical system, equation (1) can be rewritten as,

$$D = \frac{\Delta t}{\Delta \left\{ \frac{1}{[i_F(t)]^2} \right\}} \times \frac{\pi}{(nFAC)^2} \quad (2)$$

In chronoamperometry, a step function from 0.2V to -0.6V (vs. Ag/AgCl) was applied at time zero. The current were sampled per 0.01s from t=0.6s to t=20s. From the slope of  $1/i_F^2$  vs.  $t$  and equation (2), the effective diffusion coefficient in the system with 20 $\mu$ g/ml of TNT in the presence of buffer (negative control), VLP-1cys (negative control) or VLP-bp-TNT (binding agent) were derived, respectively (Table S1). The derived diffusion coefficient in the presence of binding agents was about 5-fold lower than the negative control experiment using buffer.

**Table S1**  $1/i_F^2$  vs.  $t$  slope and effective diffusion coefficient in the system

Sample	Slope of $1/i_F^2$ vs. time ( $A^{-2}s^{-1}$ )	R-square of the slope	Effective diffusion coefficient ( $cm^2s^{-1}$ )
Buffer (negative control)	$4.92 \times 10^{10}$	0.990	$5.70 \times 10^{-6}$
VLP1cys (negative control)	$6.38 \times 10^{10}$	0.976	$4.40 \times 10^{-6}$
VLP-bp-TNT (binding agent)	$2.57 \times 10^{11}$	0.998	$1.09 \times 10^{-6}$

#### Calculations of Faradaic peak current ratio in the presence of VLP-1cys negative control and VLP-bp-TNT binding agent

From the results of chronoamperometry and the above calculation, the ratio of Faradaic peak current in presence of VLP-1cys negative control and VLP-bp-TNT binding agent at a 20 $\mu$ g/ml TNT concentration was estimated as:

$$Current\ Ratio_{estimation-20\mu g/ml} = I_{control}/I_{binding\ agent} = (D_{control}/D_{binding\ agent})^{1/2} = (4.4/1.09)^{1/2} = 2.01$$

From the experimental results shown in Fig. 7(a), the Faradaic current ratio in the experiments with 0.6mg/ml of VLP-1cys and 0.2mg/ml of VLP-bp-TNT was calculated as:

$$I_{control-10\mu g/ml} = 65.5 - 36.65 = 28.85 \mu A,$$

$$I_{binding\ agent-10\mu g/ml} = 49.6 - 37.25 = 12.35 \mu A$$

$$Current\ Ratio_{10\mu g/ml} = 28.85/12.35 = 2.34$$

From the slope of current between TNT concentrations of 8 $\mu$ g-10 $\mu$ g, the Faradaic current ratio in the experiments with VLP-1cys and VLP-bp-TNT was estimated as:

$$I_{control-20\mu g/ml} = 28.85 + 5 \times (65.5 - 60.8) = 52.35 \mu A,$$

$$I_{\text{binding agent-}20\mu\text{g/ml}} = 12.35 + 5 \times (49.6 - 46.9) = 25.85 \mu\text{A}$$

$$\text{Current Ratio}_{20\mu\text{g/ml}} = 52.35 / 25.85 = 2.03$$

Therefore, the current ratio calculated from the experimental data agrees well with the estimation of the diffusion coefficients as characterized by chronoamperometry and the Cottrell equation.

### Experiment setup and reagents for the beaker-scale VLP-based electrochemical sensor

The standard TNT stock solution in 1000 $\mu\text{g/ml}$  concentration was purchased from Cerilliant Corporation, USA. The TNT working solution with concentration of 2 $\mu\text{g/ml}$ -10 $\mu\text{g/ml}$  was obtained by diluting the 1000 $\mu\text{g/ml}$  standard TNT stock solution with 0.1M NaCl and 0.01M sodium phosphate buffer supporting electrolyte in the electrochemical setup. The total amount of working solution in each experiment with varying concentrations of TNT and VLP binding agents was set to be 5ml. Gold working electrode with 56mm<sup>2</sup> area was microfabricated on a silicon substrate with a 500nm of silicon oxide passivation layer. Platinum wire counter electrode (CHI105) and Ag/AgCl reference electrode (CHI111) were purchased from CH Instrument, INC, USA. The 3-electrode electrochemical cell was connected and tested using a CHI660D electrochemical workstation (CH Instrument). Square wave voltammetry was used as the testing technique with a square wave amplitude of 25mV, a step voltage of 4mV and a frequency of 50Hz. The potential range scanned in the square wave voltammetry was set to be -0.3V~-0.7V (vs. Ag/AgCl) to locate the reduction peaks of nitro groups (-NO<sub>2</sub>) in TNT molecules. 20 minutes of nitrogen purging was performed before each experiment. The beaker scale electrochemical setup and configurations were shown in Fig. S2.

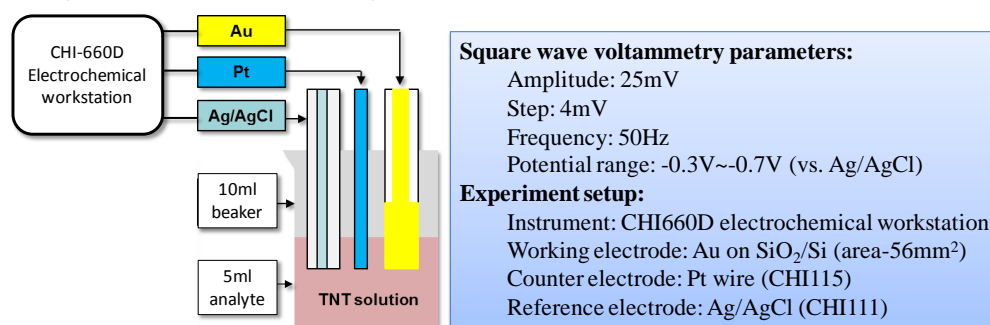


**Fig. S2** Beaker-scale electrochemical sensing platform setup and parameters of square wave voltammetry

### Fabrication and optimization of the microscale VLP-based electrochemical sensor

The microscale electrochemical sensors were fabricated on silicon wafers. Chrome and gold layers (20 nm and 200 nm, respectively) were deposited on a SiO<sub>2</sub> coated silicon substrate using E-beam evaporation. The wafers were patterned and etched after metal deposition using photolithography and wet chemical etching. The on-chip gold microelectrodes were used as working, counter and pseudo-reference electrodes. A layer of polydimethylsiloxane (PDMS) was used to form wells on the chip for the analyte introduction. After PDMS curing, holes with a 4 mm diameter were

punched in PDMS followed by alignment and bonding on the diced chip. This formed an electrochemical reaction chamber with a volume of 30 $\mu$ l. Three sensors with identical design were tested in a multiplexed configuration to obtain three independent experimental results (Fig. S3).

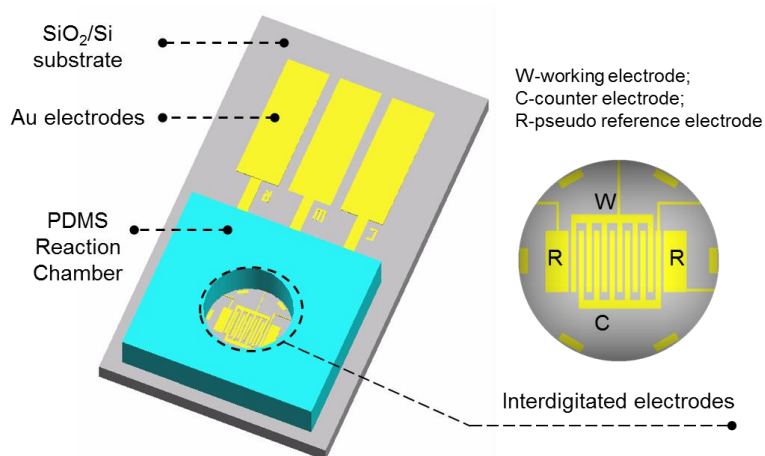


**Fig. S3** Schematic of the microscale electrochemical sensor design

**Supporting References:**

- S1. A. D. Brown, L. N. Naves, X. Wang, R. Ghodssi, and J. N. Culver, *Biomacromolecules*, 2013, **14**, 3123-3129;
- S2. B. Singaravelan, B. R. Roshini, and M. Hussain Munavar, *Journal of Bacteriology*, 2010, **192**, 6039-6044;
- S3. A.J. van Stroey and L.J.J. Janssen, *Analytica Chimica Acta*, 1993, **279**, 213-219;